



Application of isotopic labels optimised for large scale plot experiments

Arne Tenspolde¹ · Kristina Kleineidam² · Christoph Müller^{2,3} · Nicole Wrage-Mönnig¹

Received: 25 January 2023 / Revised: 1 May 2023 / Accepted: 3 May 2023
© The Author(s) 2023

Abstract

Isotopic tracer methods using ^{15}N or other isotopes provide insights into the sources and underlying N transformations leading to N_2O emissions from agricultural soils. However, homogeneous labelling of naturally structured soil in the field is challenging since macropore flow must be avoided while the application must be performed in a limited timeframe. Therefore, we tested the infiltration pattern of several application methods and consequently developed drip application (DA) for larger scales using individual dropper bottles. We performed a proof of concept test, followed by an evaluation experiment *in-situ* with a manual sprinkler as control at an undisturbed grassland site using $^{15}\text{NH}_4^{15}\text{NO}_3$ (80 kg N ha⁻¹, 10 at.%, 15 mm precipitation equiv.). $^{15}\text{N-NH}_4^+$ and $^{15}\text{N-NO}_3^-$ recovery rates and corresponding correlation coefficients were calculated to examine horizontal and vertical homogeneity. The proof of concept test showed the negative effect of very dry topsoil on homogeneous infiltration. DA achieved significantly larger ^{15}N recovery rates than sprinkler application and led to a more homogeneous horizontal label distribution. For DA, coefficients of variation of ^{15}N recovery rates were smaller than with sprinklers for most depths, yet for both methods ^{15}N recovery rates especially of $^{15}\text{N-NH}_4^+$ decreased vertically. Besides optimised label distribution, the DA method offers high flexibility in application patterns while offering reproducibility, feasibility and a reasonable application speed also at undisturbed sites at the plot scale. Moreover, DA causes no change in soil structure or soil diffusivity. Thus, the drip application method was found suitable for tracer application to field sites.

Keywords Stable isotope · Nitrous oxide · Drip application · Label · ^{15}N · Syringe

Introduction

Agricultural soil treated with mineral and organic N fertilizer is a major source of anthropogenic nitrous oxide (N_2O) emissions (Hartmann et al. 2013; Syakila and Kroeze 2011; Thompson et al. 2019). While nitrification and denitrification are major microbial pathways for the production of N_2O in soil (Bowden 1986), there are also other important microbial and chemical sources that are challenging to distinguish as they can take place simultaneously (Heil et al. 2015; Stein 2019; Wrage-Mönnig et al. 2018). Several isotopic tracer methods have been developed to differentiate among pathways (Wrage-Mönnig et al. 2018; Zaman et al. 2021). Common methods are the triple labelling approach (Müller et al. 2014), the dual-isotope method (Kool et al. 2011; Zaman et al. 2021) or the ^{15}N gas flux method (^{15}NGF) (Siegel et al. 1982; Well et al. 2019). All these isotopic methods assume homogeneous distribution of the applied ^{15}N (triple labelling and ^{15}N gas flux method) (Lewicka-Szczebak and Well 2020) and ^{15}N and ^{18}O tracers (dual-isotope method) in the

✉ Arne Tenspolde
arne.tenspolde@uni-rostock.de

Kristina Kleineidam
kristina.kleineidam@bot2.bio.uni-giessen.de

Christoph Müller
christoph.mueller@bot2.bio.uni-giessen.de

Nicole Wrage-Mönnig
nicole.wrage-moennig@uni-rostock.de

¹ Grassland and Fodder Sciences, Faculty of Agricultural and Environmental Sciences, University of Rostock, 18059 Rostock, Germany

² Institute of Plant Ecology, Justus Liebig University Giessen, 35392 Giessen, Germany

³ School of Biology and Environmental Science and Earth Institute, University College Dublin, Dublin, Ireland

examined soil volume, respectively. In laboratory incubation experiments, this is achieved through intensive mixing of sieved soil with the tracer solution, which is, however, not comparable with undisturbed soils and intact soil structure. Tracers have also been applied with multiple needle injections in different positions and depths into intact soil cores (Davidson et al. 1991) using peristaltic pumps (Buchen et al. 2016), or by continuous application while pushing the needle into the topsoil (Sgouridis et al. 2016). In other studies, side-port cannulas have been used instead of needles to prevent blocking (Wu et al. 2011). Multiple needle injections indicated a more homogeneous ^{15}N label distribution compared to label application to sieved soil followed by repacking (Lewicka-Szczebak and Well 2020), while preserving most of the soil structure.

Further improvements in our understanding of soil N transformation processes can be expected from field experiments with undisturbed soil where soil aggregates are intact (Barnard et al. 2005; Sextone et al. 1985) and plant effects occur (Müller and Clough 2014). However, the combination of heterogeneity of undisturbed soils, the size of field experiments and a certain speed requirement for label application (Moser et al. 2018; Zaman et al. 2021) make a homogenous tracer application in the field challenging.

Fast application can be achieved by watering cans (Moser et al. 2018), however, neither this nor the application by sprayer led to a homogeneous tracer distribution in a field test, indicated by large horizontal and vertical variation (Berendt et al. 2020). Also, losses of tracer solution by runoff and preferential flow were observed with watering cans, resulting in a recovery rate of only 67 % (82 % sprayer), whereas more tracer solution was retained by plant leaves in the sprayer treatment (Berendt et al. 2020). Higher vertical than lateral infiltration speeds by preferential flow through macropores are supported by water repellency and high clay contents (Jarvis 2007; Nimmo 2012). Under ponding conditions, which are more prevalent with rapid application rates, flow converges within a shallow distribution zone towards conducting flow channels, while avoiding large parts of the pore space (Flühler et al. 1996; Jarvis 2007; Ritsema and Dekker 1995). This infiltration pattern leads to deep infiltration (> 20 cm depth), resulting in a very diverse soil volume that is labelled, making ^{15}N signatures of produced N_2O challenging to interpret (Berendt et al. 2020). As a consequence, decreasing the application rate should generally lead to less preferential flow (Anderson and Bouma 1977; Elrick and French 1966; McLeod et al. 1998; Radulovich et al. 1992; Seyfried and Rao 1987).

So far, there is no approved method for homogeneous tracer application *in-situ* at the plot scale. Thus, our objective was to develop an application technique enabling a homogeneous tracer infiltration and distribution in undisturbed, vegetated soil in an acceptable time frame at the

plot scale. On this basis, we initially tested four methods at the laboratory scale on intact soil blocks, three methods that promote infiltration by capillary forces (wick and drip application, respectively) and one control method imitating application by a small watering can as the easiest scalable method so far. We hypothesized that a) the methods promoting capillary transport would result in better recovery, as runoff and deep infiltration should be reduced and that, b) point application would reduce retention by plant leaves. Furthermore, comparing the capillary methods, we hypothesized that wick application results in a cylindrical infiltration pattern from the wick outwards into the soil matrix while drip application leads to a half spherical infiltration pattern, with the dripping point as spherical centre. Drip application should therefore result in a better recovery in the topsoil. In the pre-test, we also assessed practicability and scalability, including application duration as decisive factor to choose a method for further implementation.

Based on the results of this pre-evaluation, we further developed the drip application technique to a suitable method applicable for ^{15}N tracer solutions at the plot scale. Several key points for a successful large-scale drip application were identified: sufficiently long application duration, liquid volume applied via single reservoirs for each dripping point at a constant dripping speed, and a cost-effective design with as few parts as possible to simplify the construction. Two subsequent *in-situ* experiments were conducted using $^{15}\text{NO}_3$ / $^{15}\text{NH}_4$ to test functionality and effects on label distribution and recovery compared to application with a small sprinkler according to Zaman et al. (2021). Generally, we expected drip application to lead to better horizontal homogeneity than sprinkler application, yet with increasing variability in increasing distance to the drip points. As NH_4^+ is less mobile than NO_3^- in the soil matrix, notably in clay-rich soils due to adsorption, we expected a larger heterogeneity of $^{15}\text{NH}_4^+$ in both horizontal and vertical directions (Sollins et al. 1988).

Materials and methods

Laboratory pre-tests of application methods using blue dye

Application methods and test procedures

The application methods were tested with blocks of soil extracted from a meadow at the experimental station of the University of Rostock (54° 3' 42.85" N, 12° 5' 1.07" E). Long-term extensive cultivation by mowing assured a well-structured loamy sand (79 % sand, 16 % silt, 3 % clay, 2 % organic matter) with a large density of earthworms and their burrows. Soil conditions and type were chosen to allow rapid

infiltration and meaningful distribution patterns being superimposed by the disruptive element of macropore flow. A total of 10 intact soil blocks of 0.09 m^2 each ($0.3 \text{ m} * 0.3 \text{ m}$) were collected with a depth of 25 cm. The soil blocks were dried in a windowless but lighted room for 7 days with covered sides and bottom and open top at about 19°C before starting the experiments. Thereby, the soil was dried to 25 vol % water content ($\text{SD} \pm 6\%$), minimizing the blocking effect of pore water (Berendt et al. 2020). Soil moisture was measured at the day of application three times per soil block with the ML3 ThetaKit (Delta-T Devices®). Before

application, vegetation was cut by hand to a height of 1.5 cm to reduce loss of solution onto plant leaves.

To compare four application methods, we used the standard Brilliant blue method: 0.54 l 'Brilliant blue FCF' dye (E133) solution (7 g l^{-1}) were applied to each soil block (corresponding to 6 l m^{-2} precipitation) to visualize infiltration patterns that can be analysed by image processing software (Flury and Flühler 1994). We compared (i) Wick application ($n = 3$) (Fig. 1A), (ii) Drip application along a vertical Macropore (drip application (M), $n = 3$) (Fig. 1B), (iii) Drip application ($n = 1$) (Fig. 1C), and (iv) Control application

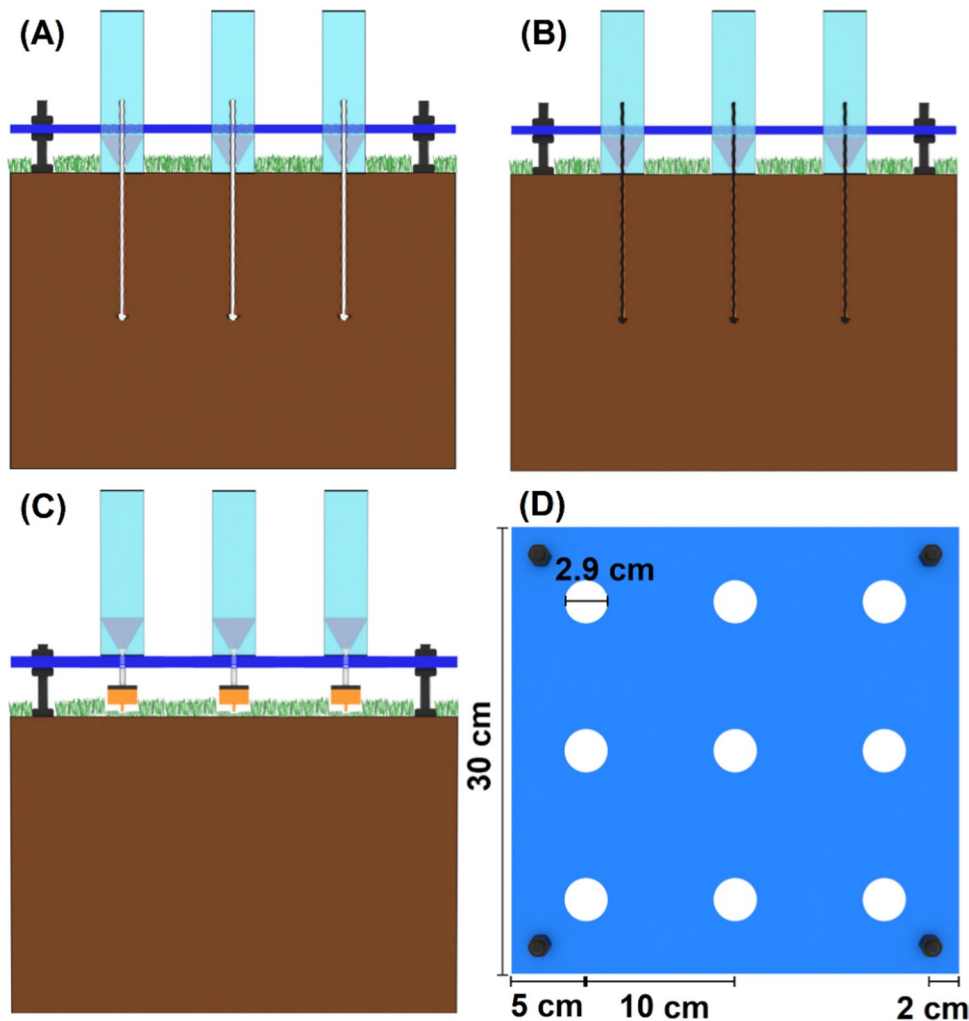


Fig. 1 Details on the application setups used in the pre-test with blue dye at a laboratory scale. **A)** Side view of application by 3 mm wicks pushed 10 cm deep into the topsoil. The wicks end in reservoirs made from centrifuge tubes (Brand™ 114821 50 ml with base) held in place by a $30 \text{ cm} \times 30 \text{ cm} \times 6 \text{ mm}$ acrylic sheet. The acrylic sheet is fixed approximately 3 cm above ground by height-adjustable stands made from threaded rods ($\text{Ø} 8 \text{ mm}$) and three nuts each. The gap between the wick and reservoir was sealed with glue pads (UHU® Patafix). **B)** Side view of drip application with vertical macropores (drip application (M)). Unconductive glass fibre wicks ($\text{Ø} 2 \text{ mm}$) were pushed 10 cm into the topsoil, creating a vertical macropore

below the reservoirs. The gaps between the reservoir and wicks were incompletely sealed allowing a slow dripping onto the soil below the reservoirs. The reservoirs were stabilized with an acrylic sheet, similar to 1A. **C)** Side view of the drip application. Drip outlets were connected via PVC tubes (2 cm) to the bottom of each reservoir. The gap between the PVC tube and reservoir was sealed with a glue pad. The reservoirs were stabilized with an acrylic sheet, similar to 1A. **D)** Top view of an acrylic sheet ($30 \text{ cm} \times 30 \text{ cm} \times 6 \text{ mm}$) for one soil block with 9 holes ($\text{Ø} 29 \text{ mm}$) to hold the reservoirs and four stands at each corner

using a syringe for surface application ($n = 3$). For methods (i)-(iii), the dye solution was equally distributed over 9 infiltration points arranged in a 10 cm square grid (Fig. 1D).

For the wick application, a 3 mm thick irrigation wick with a cotton core was pushed 10 cm deep into the topsoil from above using a stainless-steel tube (4.4 mm outer and 3.6 mm inner diameter (\emptyset)) (Fig. 1A). A knot in the wick at the bottom tip of the stainless-steel tube served as anchor when the tube was removed. To speed up application, we first attached nine tubes in a 10 × 10 cm grid to a 30 cm × 30 cm × 4 mm steel plate and tried to push them all in simultaneously. Yet, a minor deviation from the perfect right angle between tube and plate or a small obstacle caused the tubes to bend. Therefore, we decided to apply each wick individually. Aboveground, each wick ended in a 25 ml reservoir (Brand™ 114821 50 ml centrifuge tubes with base, shortened at the top to a capacity of 25 ml), with a 5 mm \emptyset hole drilled into the tip of the reservoir and the connection sealed off by glue pad (UHU Patafix). The reservoirs were stabilized by a plate of acrylic sheets with fitting holes and height-adjustable stands made from 8 mm threaded rods (Fig. 1D).

For the drip application (M), similar to the wick application, a 2 mm wick with fiberglass core was pushed 10 cm into the topsoil using a stainless-steel tube (3 mm outer and 2 mm inner \emptyset) that was subsequently removed (Fig. 1B). The 2 mm wick was non-conductive. The gap between wick and reservoir was not perfectly sealed to allow slow dripping of the solution along the wick onto the vertical macropore that was created when the wick was pushed in. For the drip application, drippers (Esotec GmbH, part of solar irrigation set WaterDrops; Fig. 1C) were attached to the bottom of a PE tube (4 mm inner and 7 mm outer \emptyset). The top facing end of the tube was positioned at the bottom of a reservoir and sealed with glue pads. Furthermore, a small piece of glue pad (in the size of a rice grain) was introduced inside the drip outlets to

further decelerate the dripping speed. Pre-tests showed that otherwise, application would have been finished in less than 2 minutes. For methods (i)-(iii), the reservoirs were filled three times consecutively with 20 ml of the dye

Solution and the duration of each emptying was measured. For method (iii), as only three drippers were available, application was performed consecutively for each third of the soil surface.

The control application (method (iv)) with a syringe should mimic application with a small sprinkler (Zaman et al. 2021), but with greater accuracy to avoid losses at the edges of the soil blocks. For this, the block was divided into three sections (each 10 cm × 30 cm) with the help of a folding rule and marked with a thin rope. A syringe (100 ml) filled with 0.09 l of dye solution was emptied as evenly as possible in serpentine lines over each section.

Application was repeated after turning the position of the soil block by 90°.

Determination and assessment of the blue dye distribution

One hour after finishing application, soil blocks were cut into profiles along infiltration points ((i)-(iii)) or along the centre line of each section (iv). Both sides of each profile were photographed from a distance of 25 cm using a folding rule for normalization of pictures. Constant lighting conditions were provided by an almost continuous light source along one wall facing the profiles inside a windowless room. Care was taken to take the photos at the same position and with the same angle.

With the image processing software ImageJ, blue coloured areas were extracted using the same thresholds of hue (68-189), saturation (0-255) and brightness (10-235) and were subsequently changed into HSB Stacks (8 bit). To compare vertical distribution homogeneity, different depth sections (five 2.5 cm steps from 0-12.5 cm and a sixth from 12.5-20 cm) per 30 cm wide grayscale image of saturation were selected and integrals calculated. For horizontal distribution homogeneity and comparison of the relative coloration intensity (RCI, see below), ten 3 cm wide and 20 cm deep parts of the same grayscale images were selected and integrals calculated.

Calculations and Statistics

Integrals were normalized with the ‘pixels per centimetre’ values derived from the photographed folding rules (Irfan View). The RCI was calculated from these integrals as percentage of maximum possible coloration. This maximum possible coloration was assumed equivalent to the amount applied to each soil block distributed evenly throughout the top 10 cm of soil. It was determined using 250 g of dried and crumbled soil (24 h at 105 °C) from the experimental station rewetted with 52.43 ml of distilled water ($\hat{=}$ 25 vol%) and mixed manually with 12.56 ml of 7 g l⁻¹ ‘Brilliant blue FCF’ (E133) solution. The coloured soil was filled in a flat container and the surface was photographed with the same light conditions as the soil profiles after infiltration. Coloured areas were extracted and converted to HSB-Stacks (8bit) as above, with a threshold (10-199) set to avoid underexposed areas. Nine random areas (1 cm²) of the resulting saturation image were selected in ImageJ and the mean coloration of the pixels within was calculated. The highest mean value was used as potential maximum coloration intensity. For the RCI values of the horizontal distribution, homogeneity, means, medians, standard deviations (SD) and coefficients of variation (CV) were calculated for each method. Normality of the data was checked with the Shapiro-Wilk-Test. Kruskal-Wallis tests and post-hoc pairwise Wilcoxon

tests (“bonferroni”) were performed to check for differences between application methods. For the RCI values of the vertical distribution homogeneity, means, medians and standard deviations were calculated. R (3.6.3) was used for statistical analyses (R Core Team 2021).

Field testing of drip application method using ^{15}N tracers

Experimental setup and materials

The drip application was tested in two *in-situ* experiments: first, a proof of concept testing the application with dropper bottles and second, an evaluation experiment (EE) comparing the drip application with the sprinkler method. Both were conducted at the Environmental Monitoring and Climate Impact Research Station Linden, University Giessen (50°31'57.5"N, 8°41'06.0"E) on a stagno-fluvic gleysol. The grassland has been unploughed for at least 100 years and fertilization has been at 40 kg N ha⁻¹ yr⁻¹ for more than 25 years (Jäger et al. 2003). The proof of concept was performed in

late September 2020 under very dry soil conditions (43.0 % WFPS) on three plots of 40 cm × 40 cm each (Fig. 2A). For each plot, 49 bottles were used. Drip outlets (Esotec GmbH, part of solar irrigation set WaterDrops) were attached to 100 ml eye dropper bottles (Low density polyethylene (LDPE)) with PE tubes (4 mm inner and 7 mm outer Ø) fed through holes drilled into the caps of the eye dropper bottles (Supplementary Fig. 1). Three-way valves (Teqler Three-way Stopcock T-135180) glued to the bottom allowed a controlled start of application (Fig. 2C, Supplementary Fig. 1). Small punched out cotton pads were introduced into the drip outlets to reduce flow. As a support structure, we used 60 cm × 40 cm × 8 mm acrylic sheets hold in place at least 15 cm above ground by two angle bars, which themselves rested on four wooden stakes at the edges of the plot fixed with double-sided tape (Fig. 2A, 2C). For each dropper bottle, one 3.5 cm wide hole was cut into the sheets by a laser cutter (Fig. 2A). The tips of the drip outlets were then around 1 cm above the soil surface to minimize both obstruction by plant leaves and blocking by soil particles (Fig. 2C). The optimal distribution of drip points is a triangular grid with dropper

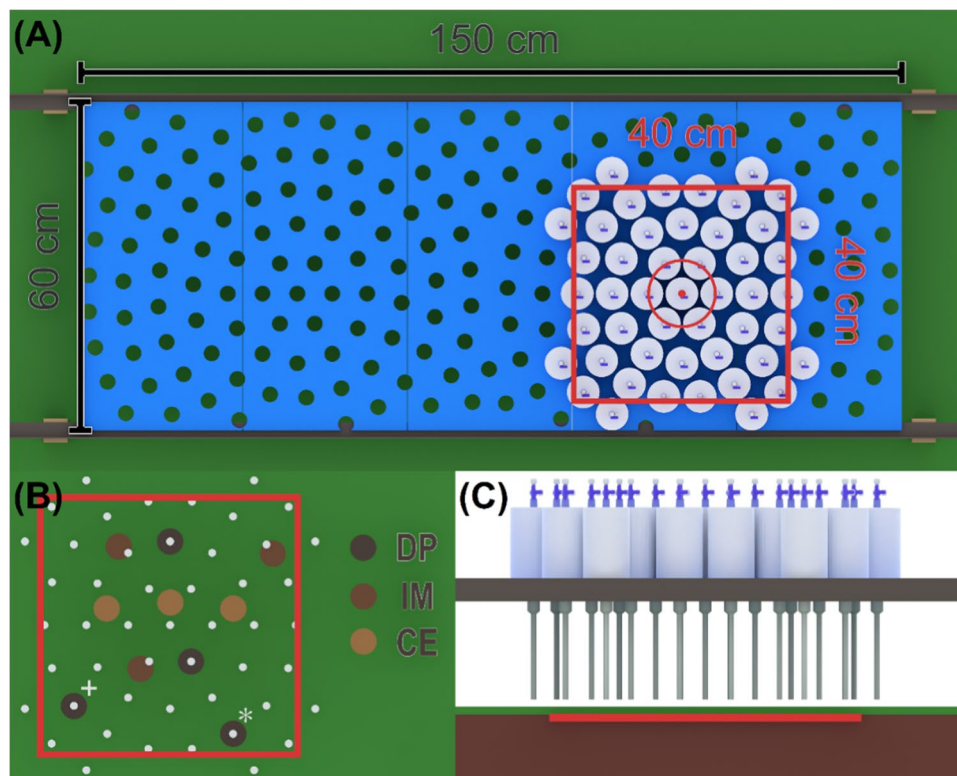


Fig. 2 A) Support structure for dropper bottles with a circular (red circle: $r_x = x \times 6.35\text{cm}$) distribution pattern of drip points and 3.5 cm wide holes for each bottle. For the proof of concept and evaluation experiments the square plot area shown (red: 40 cm × 40 cm) was equipped with 49 bottles. B) Top view of the plot area with infiltration points (white) and locations of soil samples from three different distances to infiltration points: directly below a dropper point (DP), in

the centre between three dropper points (CE) and at an intermediate position between DP and CE (IM). DP sampling location (+): proof of concept plot 1 and 2, (*): proof of concept plot 3 and evaluation experiments. C) Sideview with the dropper bottles held by an acrylic sheet with 3.5 cm holes for each bottle resting on angle bars. Bottles are held so high that the cannulas are just above ground. Three-way valves are opened to start drip application

bottles touching each other, resulting in the smallest and equal distance between all drip points. However, the separate reservoirs allow to realize also other uniform patterns. We tested a circular design (matching round greenhouse gas sampling chambers) with a centre radius of 6.35 cm (Fig. 2A), 6 drip points on the first ring and further 6 for each additional ring resulting in a consistently covered area per drip point of 0.00418 m².

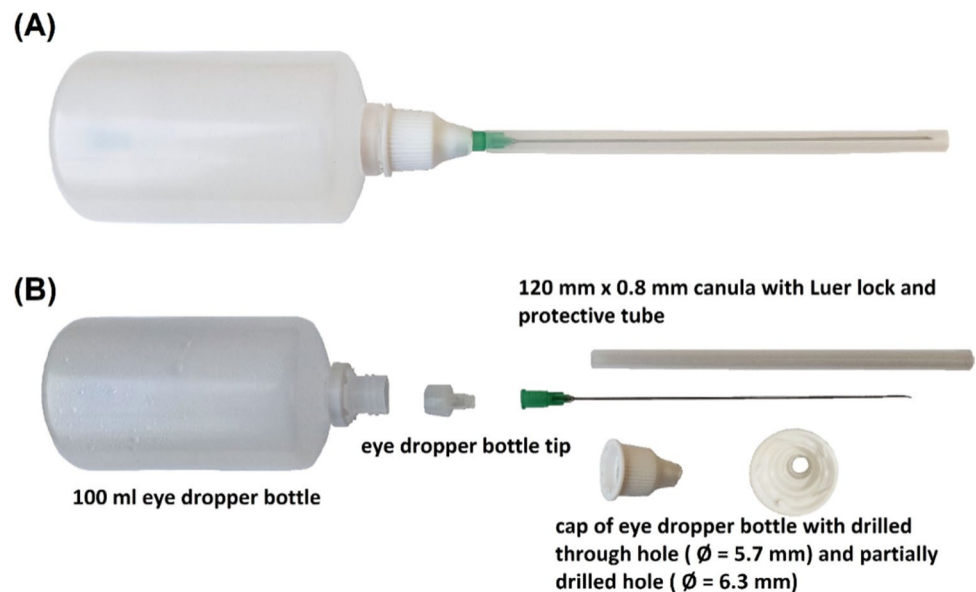
The bottles were filled with 62.5 ml double-labelled ammonium nitrate (¹⁵NH₄¹⁵NO₃, 80 kg N ha⁻¹, 10 at.%) to simulate a 15 mm rainfall event. As there were two areas available on one set of acrylic sheets, label was applied to plot 1 and 2 simultaneously and to plot 3 immediately thereafter. Two hours after the start of the application nine soil samples (Ø = 8 cm) were taken per plot to a depth of 20 cm from three different distances to infiltration points using a template: directly below a dropper point (DP), in the centre between three dropper points (CE) and at an intermediate position between DP and CE (IM) (Fig. 2B).

Additionally, each soil core was separated into five depths (0-2.5 cm, 2.5-5 cm, 5-7.5 cm, 7.5-10 cm and 10-20 cm). For all soil samples, gravimetric water content (drying at 105°C for 24 h) was measured. For extraction of mineral N, 20 g of fresh soil were shaken for 1 h in 100 ml 2M KCl in 250 ml PE bottles (Brand GmbH, Germany) and afterwards vacuum-filtered with two layers of glass fibre filters (GF 50, 125 and 90 mm Ø, Hahnemühle FineArt GmbH, Germany). Concentrations of NH₄⁺-N and NO₃⁻-N in the KCl extracts were determined by AutoAnalyser AA 3 (Seal Analytical). ¹⁵N-NH₄⁺ and ¹⁵N-NO₃⁻ abundances were determined by microdiffusion (Brooks et al. 1989; Wrage et al. 2005) and subsequent analysis on an isotope ratio mass spectrometer (IRMS) (Elementar,

Isoprime 100) coupled to an elemental analyser (Elementar, PyroCube). Measurements were calibrated for ¹⁵N abundance with sulfanilamide (nat. abundance ¹⁵N), rye flour (nat. abundance ¹⁵N) and IAEA-311 (2.05 at. % ¹⁵N). Sulfanilamide and rye flour were used as working standards, with sulfanilamide measured twice every 10 samples and rye flour three times before and after measurements.

In the evaluation experiment (EE) in early October 2020, the drip application was compared to a control method for plot experiments using laundry sprinklers according to Zaman et al. (2021). In lack of an approved method for application at plot scale the sprinkler application served as a control method. A small rainfall event (7 mm) on the day before the experiment left the soil slightly moist with a gravimetric soil moisture content of 32.4 % in the top soil layer (0 - 2.5 cm) compared to 25.2 % during the proof of concept. In the latter, the reduction of flow through the dropper bottles was still too inconsistent, leading to an adaptation for EE. To ensure a slow but steady dripping speed of the label solution on each dropper point, cannulas (BRAUN: STERICAN cannulas 21 Gx4 4/5 0,8x120 mm) instead of drip outlets were attached to 100 ml eye dropper bottles (low density poly ethylene (LDPE)) (Fig. 2C), resulting in at least 45 min of dripping for 100 ml solution (mean ~63 min, SD +/- 4.0 min, 9 replicates). One hole (Ø = 5.7 mm) was drilled though the cap and one hole (Ø = 6.3 mm) was only partially drilled though from the inside using a bench drill and wooden adapter for fixation (Fig. 3). This allowed the cannula and the protective tube included with the cannula to fit though the hole but not the Luer-Lock adapter. Thereby, a good connection of the cannula and the tip of the eye dropper bottle was achieved (Fig. 3).

Fig. 3 Final version of the bottle used for the drip application in the comparative experiment at plot scale. **A**) Assembled, ready-to-use dropper bottle. **B**) Individual components of the dropper bottle with the bottle, tip, cannula, protective tube of the cannula and cap of the eye dropper bottle



With the drip and sprinkler application, label was applied to one plot (40 cm x 40 cm) using the same parameters as in the proof of concept (15 mm precipitation equivalent, 80 kg N ha⁻¹, double ¹⁵N-labeled NH₄NO₃ at 10 at.%). Sampling, sample preparation and analysis were performed as outlined above, except that only four depths down to 10 cm were sampled. For background soil moisture and NH₄⁺-N and NO₃⁻-N concentrations, three soil samples were taken for each experiment from the area around the plots and separated into the respective depths.

Calculations and statistics

The recovered amount of ¹⁵N was calculated for each sample and aggregated to recovery rates in two ways. To investigate the horizontal homogeneity, the recovery rate of the hole sampling depth (0 -10 cm) of each soil sample was calculated as percentage of applied ¹⁵N. For the vertical homogeneity the ¹⁵N recovery rate for each 2.5 cm layer was calculated as a percentage of the theoretical value attained assuming completely homogeneous label distribution in the top 10 cm. The theoretical value was calculated as the applied ¹⁵N divided by four for the four equivalent soil layers that were sampled. A vertically homogeneous label distribution is reached at a 100 percent recovery rate for all four depth layers, while values below and above are possible.

Per treatment, means, standard deviations (SD) and coefficients of variation (CV) were calculated for these recovery rates aggregated for either soil layers (horizontal), sampling points (vertical) and sampling points separated into the three distances to infiltration points by selecting corresponding recovery rates for the calculation. Normality of the data was checked with the Shapiro-Wilk-Test. As most data was not normally distributed, Kruskal-Wallis tests and post-hoc Wilcoxon tests (“bonferroni”) were performed to check for differences between application methods and experiments. R (3.6.3) was used for statistical analysis (R Core Team 2021).

Table 1 Soil moisture increase due to application and relative colour intensity (RCI) values measured in the laboratory pre-test of different application methods using blue dye: means with standard deviations (SD), medians and coefficients of variation (CV). WA: Wick application, DM: Drip application with vertical Macropore (M), DA: Drip

Application Method	WA	DM	DA	CA
Application time (minutes)	758 ± 466	84 ± 63	28 ± 24	6 ± 1
Mean soil moisture increase (vol %) ± SD	1.8 ± 8.1	4.9 ± 7.8	12.5 ± 18	6.1 ± 9.1
Mean RCI (%) ± SD	92.0 ± 75.8 ^{bc}	98.8 ± 71.3 ^c	65.4 ± 36.8 ^b	47.6 ± 28.9 ^a
Median RCI (%)	74.3	93.6	62.9	43.1
CV RCI (%)	82.3	72.2	56.3	60.7
Median RCI (%) t > 45min ± SD	-	96.5 ± 73	92.0 ± 38.9	-

Results

Laboratory tests of application methods

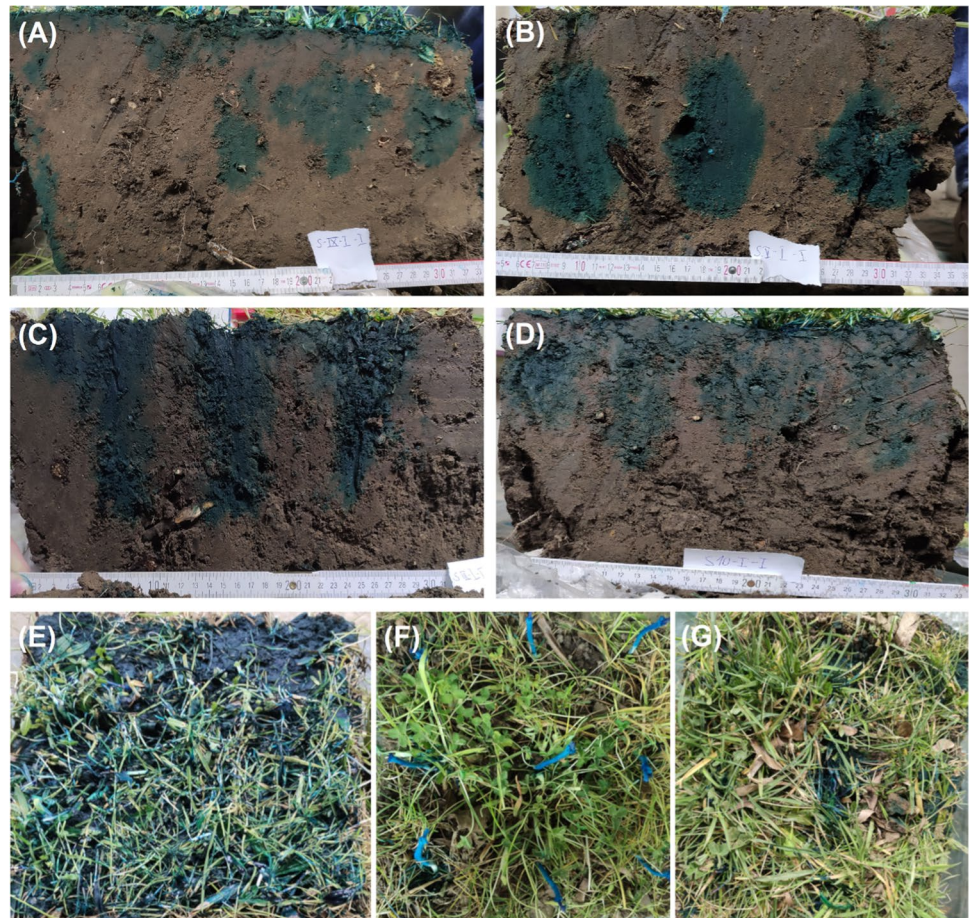
The comparison of application methods at the laboratory scale revealed that the control application was by far the fastest techniques, taking only 6 minutes (Table 1). The drip application (M) took on average 84 and the drip application 28 minutes. Both methods showed clearly varying application times (high SD and CV for drip application (M) and drip application, respectively), caused by variable dripping speeds within one method among the different reservoirs as well as within the same reservoir among partial applications. Infiltration by wick application took on average 758 minutes (2 - 24 hours).

Large differences between profiles in staining patterns and in affected soil surface area were observed (Fig. 4A 4D). While the control application showed a rather spotty distribution of colour, the wick application resulted in a pear-shape coloration centred around the end of the wick. Interestingly, the wick was only coloured on the inside and most colour seems to have left near the knot end. The drip application (M) application led to a downward bulged cone shape with sharp edges and the deepest colour. The drip application resulted in a lighter colour, but large parts of the soil were affected, especially in the top layers (Fig. 4A 4D). Application with the control application resulted in an extensive staining of soil surface and plants compared to spot colouration around infiltration points with the wick application and drip application (M) (Fig. 4E 4G).

Comparing mean RCI of vertical soil areas (0 - 20 cm), this was significantly smallest for the control application (drip application: $p = 0.004$, drip application (M): $p < 0.001$, wick application: $p < 0.001$, Table 2), followed by drip application, wick application and drip application (M). In drip application (M) and wick application, many

application and CA: Control application. Also, median (+/- SD) RCIs values for application times longer than 45 minutes are shown for drip application (M) and drip application. Different superscript letters indicate statistically significant differences among application methods ($\alpha = 0.05$). For further explanation of methods, see text

Fig. 4 Soil profiles of sods after application of blue dye solution in the pre-test at laboratory scale with **A)** Control application, **B)** Wick application, **C)** Drip application with Macropore (**M**) and **D)** Drip application and top view onto sods after application with **E)** Control application, **F)** Wick application, **G)** Drip application



values were found at or even above 100% RCI due to the concentration of colour in small areas. Slower application by dripping increased the median RCI, particularly in drip application: If the RCI for drip application was calculated only for drip points with application times longer than 45 minutes, the RCI of drip application (M)

was not significantly larger than that of drip application ($p_{all} = 0.032$, $p_{t>45} = 0.520$) (Table 1).

The control application and the drip application showed the smallest horizontal variation (CV) of RCI (Table 1). The vertical distribution of RCI (Fig. 4) mirrors the staining patterns observed. While the RCI decreased with depth

Table 2 Application time, soil moisture increases due to application, mineral N concentrations and ^{15}N recovery rates of applied ^{15}N (0–10 cm depth) of the proof of concept and evaluation (EE) ^{15}N field experiment at plot scale: Shown are means and standard deviations (SD), and coefficients of variation (CV). DA (PoC): drip application

Method	DA (PoC)	DA (EE)	SA (EE)
Application time (minutes)	45–84	42	8
Soil moisture increase (%)	7.2 ± 10.1	8.5 ± 5.6	5.9 ± 6.5
$\text{NH}_4^+\text{-N}$ (mg kg ⁻¹)	10.5 ± 13.1	20.8 ± 46.7	36.3 ± 117.7
$\text{NO}_3^-\text{-N}$ (mg kg ⁻¹)	18.4 ± 14.8	13.6 ± 12.5	9.3 ± 8.2
$^{15}\text{NH}_4^+$ Recovery (%) (0–10 cm)	11.0 ± 13.9 ^a	35.4 ± 33.1 ^b	12.0 ± 20.7 ^{ab}
$^{15}\text{NO}_3^-$ Recovery (%) (0–10 cm)	39.9 ± 29.7 ^a	28.0 ± 12.0 ^a	14.0 ± 8.7 ^b
CV $^{15}\text{NH}_4^+$ (%) (horizontal)	127	93	173
CV $^{15}\text{NO}_3^-$ (%) (horizontal)	74	43	62

in the proof of concept on very dry soil, DA (EE): improved drip application in the comparative experiment on slightly wetter soil, SA: sprinkler application as control method in EE. Different superscript letters indicate statistically significant differences among application methods ($\alpha = 0.05$)

for the control application, it was largest at depth for the wick application. The drip applications showed largest RCIs for the top layers, decreasing with depth. Yet for the top 7.5 cm, RCIs for drip application and drip application (M) were relatively stable with a relative standard deviation of 24 % and 26 %, respectively (control application 46 %). Again, the wick application and the drip application (M) led to a large number of values above 100%.

Field testing of drip application method

Application times

In the proof of concept, the drip application took between 45 and 84 minutes per plot. With the adapted design in EE, drip application was finished after 42 minutes. The sprinkler application was much faster taking only 8 minutes. Gravimetric soil moisture increased significantly for all methods (Table 2).

^{15}N recovery rates

In the proof of concept, 11.0 % (± 13.9 %) of $^{15}\text{N-NH}_4^+$ and 39.9 % (± 29.7 %) of $^{15}\text{N-NO}_3^-$ was recovered after the drip application (Table 2). In EE, the mean ^{15}N recovery rate in the soil to 10 cm depth was significantly larger for the drip application (28 % ± 12.0 %) than for the sprinkler application (14.0 % ± 8.7 %) concerning $^{15}\text{N-NO}_3^-$ ($p = 0.031$) but not significantly different regarding $^{15}\text{N-NH}_4^+$ (35.4 % ± 33.1 % vs 12.0 % ± 20.7 %; $p = 0.063$) (Table 2). With drier topsoil conditions during the proof of concept, the mean $^{15}\text{N-NO}_3^-$ recovery rate with the drip application was not significantly different from that in wetter conditions (drip application in EE) ($p = 0.667$, Table 2), but significantly larger than with the sprinkler application (EE) ($p = 0.012$). However, for $^{15}\text{N-NH}_4^+$, the recovery rate was significantly smaller for drip application in the proof of concept than for drip application in EE ($p = 0.011$, Table 2) and similar as for the sprinkler application ($p = 0.914$).

Horizontal homogeneity

Comparing the horizontal homogeneity of all samples of the proof of concept and EE (bulk samples from 0 – 10 cm), CVs of recovery rates of both $^{15}\text{N-NH}_4^+$ and $^{15}\text{N-NO}_3^-$ were smallest for the drip application (EE, 0.93 and 0.43, respectively; Table 2). For the drip application of the proof of concept, the CV of $^{15}\text{N-NH}_4^+$ recovery rates were smaller than for the sprinkler application (EE) (1.27 vs 1.73) but not the CV of $^{15}\text{N-NO}_3^-$ recovery rates (0.74 vs 0.62, Table 2). Among different sampling locations in EE (DP, IM and CE), no significant differences in ^{15}N recovery rates could be observed (Fig. 5A, 5B).

Vertical Homogeneity

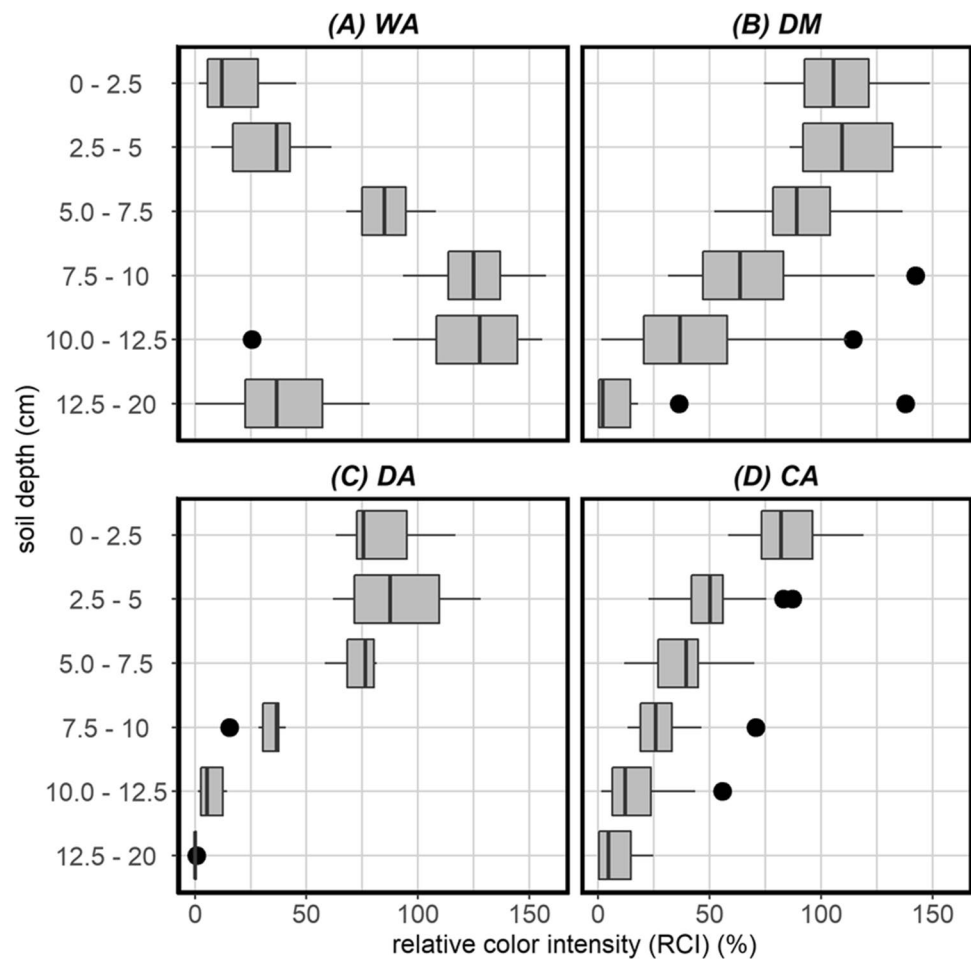
Concerning the vertical homogeneity of label application in the proof of concept, the drip application achieved highest recovery rates in the top layer (0 – 2.5 cm), with 22 % and 62 % for $^{15}\text{N-NH}_4^+$ and $^{15}\text{N-NO}_3^-$, respectively, of the recovery rate expected with a homogeneous label distribution throughout the upper 10 cm (Fig. 5C, 5D). Also, for EE, the largest recovery rates were found in the topsoil, where the drip application achieved significantly larger recovery rates of $^{15}\text{N-NH}_4^+$ and $^{15}\text{N-NO}_3^-$ compared to the sprinkler application (0 – 2.5 cm), with 140 % (drip application; rates larger than 100% indicate a concentration of label in this layer rather than the homogeneous distribution of label over 10 cm depth assumed for calculating recovery) to 25 % (sprinkler application) ($p = 0.028$) and 65 % (drip application) to 30 % (sprinkler application) ($p = 0.012$) for $^{15}\text{N-NH}_4^+$ and $^{15}\text{N-NO}_3^-$, respectively (Fig. 5C, 5D). With deeper layers, the $^{15}\text{N-NO}_3^-$ recovery rates and especially the $^{15}\text{N-NH}_4^+$ recovery rates showed a decrease with depth for all methods (Fig. 5C, 5D). Thus, in the proof of concept, with the drip application, 65 % of the total $^{15}\text{N-NH}_4^+$ recovery was found in the top 2.5 cm versus 96 % with the drip application and 53 % with the sprinkler application in EE. Also, in case of $^{15}\text{N-NO}_3^-$, 49 % of total recovery after the drip application (proof of concept) was found in the top 2.5 cm versus 60 % after the drip application and 50 % after the sprinkler application in EE. Yet, in EE for all depths the CVs of the ^{15}N recovery rate were smaller for the drip application for both $^{15}\text{N-NH}_4^+$ and $^{15}\text{N-NO}_3^-$ compared to the sprinkler application (except for $^{15}\text{N-NO}_3^-$ in 7.5 – 10 cm).

Discussion

Laboratory pre-tests on infiltration optimization

We compared three application methods with a control application by syringe at the laboratory scale regarding the four criteria intensity and homogeneity of soil coloration, practicability and scalability. Concerning intensity of coloration, all three methods had a significantly larger RCI than the control application (Table 1), showing that they were better than the control method. Thus, slower application probably led to avoidance of preferential flow (Anderson and Bouma 1977; Elrick and French 1966; Flüher et al. 1996; Jarvis 2007; McLeod et al. 1998; Radulovich et al. 1992; Ritsema and Dekker 1995; Seyfried and Rao 1987), confirming our initial hypothesis. Other interactions such as the potential for adsorption to soil particles should have been limited by the low clay content of the soil (Ketelsen and Meyer-Windel 1999). In addition, the reduced staining of the plants on top of the soil blocks confirms that spot application can reduce

Fig. 5 Relative Colour Intensity (RCI) as percentage of maximum achievable coloration for separate soil layer depths for **A)** WA: Wick application, **B)** DM: Drip application with vertical Macropore (M), **C)** DA: Drip application, **D)** CA: Control application. Shown are box plots with the line in the boxes representing the median, the ends of the boxes showing the first and third quartiles, the ends of the whiskers indicating the largest or smallest values within a maximum distance to the box of 1.5 x the range of the box and the dots showing outliers



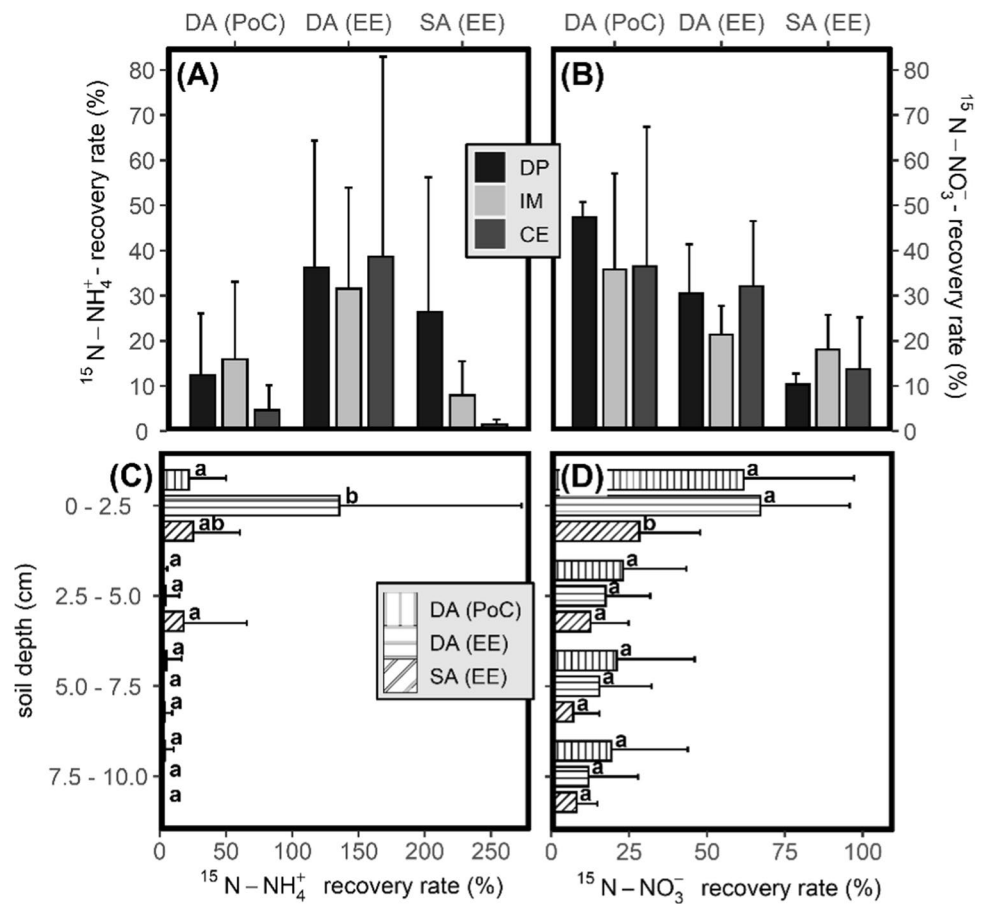
retention by plant leaves. Locally, the RCI especially of wick application and drip application (M) extended 100 %. This shows a concentration of colour in small areas, hinting at accumulation and inhomogeneous infiltration of blue dye solution. Application time as critical factor was also proven by the RCI with the drip application. While drip application (M) achieved the highest RCI, drip application could achieve a similar RCI, i.e., potential recovery rate of isotopic label when application time was sufficiently slowed down ($t > 45$ minutes).

In case of drip application (M), the vertical macropore helped to guide the solution into the soil matrix, thus facilitating infiltration into deeper soil layers than with the other methods except for the wick application. Nevertheless, we did not observe coloration in deeper areas or below the soil blocks on the floor cover, showing that flow through natural macropores was similar to that in the other improved methods. Wick application and drip application (M) were presumably slowed sufficiently not to exceed the lateral infiltration velocity (Jarvis 2007; Nimmo 2012), which is confirmed by the visually clear delineation of the staining (Fig. 4B 4C). Thus, the horizontal homogeneity of the wick application

and drip application (M), but also of the drip application can be optimized through the application of larger volumes of solution (> 6 mm precipitation equiv.) (Berendt et al. 2020) or through the closer positioning of the application points. Drip application showed the best horizontal homogeneity of all methods (Table 1), suggesting potential for precise placing of labels. Due to application from the top, some vertical inhomogeneity of both drip application and drip application (M) persisted, with largest RCI values at the surface (Fig. 4). Nevertheless, the drip application also showed an improved vertical homogeneity compared to the control application in the top 7.5 cm (Fig. 5).

Interestingly, the patterns of colour distribution varied among treatments but only partially confirmed our hypotheses of a half-spherical shape for the drip application and a cylindrical one for the wick application. Comparing vertical distribution, drip application was similar to a half-spherical distribution (Fig. 4), although this was visually not clearly recognizable (Fig. 6D). Especially the shape of the wick application was unexpected as apparently the solution was transmitted within the cotton core without wetting the outer fabric and only bridging the

Fig. 6 Recovery rates of applied $^{15}\text{N-NH}_4^+$ (A, C) and $^{15}\text{N-NO}_3^-$ (B, D) in the plot experiments after drip application in the proof of concept experiment (DA (PoC)), the evaluation experiment (DA (EE)) and after application with a small sprinkler (SA (EE)). Fig. A, B compare ^{15}N recovery rates of applied ^{15}N for soil samples (0–10 cm) taken at different distances from application points (n = 3): directly below drip points (DP), in the centre between three drip points (CE, maximal distance to application points), and at intermediate points (IM). The means of the three positions results in the ^{15}N recovery rates of Table 2. Fig. C, D show ^{15}N recovery rates for the drip and sprinkler application at different soil depths (n = 9), as percentage of applied ^{15}N if homogenously distributed in the top 10 cm (Δ^P/L for each soil layer). Shown are means \pm standard deviations



gap to the soil at the blocked end. Usually, wicks are used for upward infiltration. Thus, their fibres are arranged in a way to guide solution against gravity and to minimize losses along the wick. Due to the wick insertion with tubes, the pores were larger than the wicks, decreasing the contact area between wick and soil, which might have further decreased the loss of solution along the wick. Thus, this technique can be used to achieve a tailored placement of the tracer solution at desired depths (using different wick lengths). However, for a homogeneous distribution, wick application in several depths would be needed.

In summary, all methods improved the blue dye infiltration and distribution in the soil blocks compared to the control application. However, considering applicability, the wick application was too time-consuming for a field application. Drip application (M) was also not feasible for upscaling as the precise alignment of drip points and macropores would be very demanding. Thus, the drip application turned out to be the most promising method to enhance label application also at larger scales and was further tested *in-situ* at a field site.

Field application of the drip application method

The drip application requires more preparation time and materials compared to the sprinkler application, but achieves better results in many other aspects. Thus, the drip application with its individual bottles is a flexible method that can be adapted to the requirements of the respective experiments in terms of the arrangement of drip points, the application volume and the application pattern of different labels in a small area. Moreover, the use of templates for the positioning of the application bottles in our drip application method minimizes the influence of the user on distribution homogeneity, which is a major point with sprinkler application. Consequently, overall field applicability of the drip application is maintained or even advantageous compared to the sprinkler application, especially at the larger plot scale. However, it should be considered that our method is intended for the application on cut grassland. In case of other vegetation, its intercepting effects may require adaptations. Especially with larger plants, the solution would have to be directed past the plants to the soil to minimize interaction with the leaves.

Significantly larger ^{15}N recovery rates for the drip application than for the sprinkler application suggested smaller losses onto plant leaves and as runoff or leaching. There can be significant interceptions of precipitation in grasslands with interception capacity for shortgrass of up to 1.0 mm (Corbett and Crouse 1968; Crouse et al. 1966; Thurow et al. 1987) with highest rates at low intensity precipitation (Kinnersley et al. 1997). Because of the point application of the drip application, this should mostly be avoided, unlike with the sprinkler application. Deep percolation is increased by ponding (Bethune et al. 2008) as more solution penetrates via preferential flow through macropores (Jarvis 2007). As shown in the blue dye experiments, due to slower application rates, drip application should result in less ponding and leaching than other methods. Still, both leaching and interception might not be sufficient to explain the large differences in mean ^{15}N recovery rates of just about one third in case of $^{15}\text{N-NH}_4^+$ or half for $^{15}\text{N-NO}_3^-$ for the sprinkler application compared to the drip application (Table 2). Runoff therefore is likely another important factor explaining losses in ^{15}N label with the sprinkler application, as it has been found to be the greatest potential water loss mechanism for sprinkler irrigation systems, responsible for losses of more than 40 % (King and Bjorneberg 2011; Schneider 2000).

Moreover, runoff reduces the horizontal uniformity of application (Schneider 2000). Converging flow in the top-soil under ponding conditions with subsequent macropore flow (Jarvis 2007) contributes to heterogeneous horizontal infiltration on the centimetre scale. The results from the ^{15}N field experiments demonstrate a successful mitigation of this effect, confirming the rather homogeneous infiltration through reduced application velocity in the pre-experiment. Thus, the drip application resulted in a more homogenous horizontal label distribution than the sprinkler application (Table 1). This can also lead to a better separation of different labels in the soil when applied in close proximity. Additionally, despite the point application of the drip application, we found no significant differences in average ^{15}N recovery rates with increased distance to the drip points, which indicates sufficient lateral flow including label transport (Fig. 5A, 5B). This also implies that the applied solution volume was sufficient to reach the intermediate soil volume (Radulovich et al. 1992). Smaller soil samples (in diameter) might have resulted in larger measured heterogeneity of the recovery rate and significant differences among sampling locations. This could be further tested in future studies.

We further observed that horizontal homogeneity of the drip application benefitted from some precipitation the day before application, probably alleviating water repellency and consequently macropore flow due to a very dry top soil (Doerr et al. 2000). Nevertheless, wet soil may also have a negative effect on homogeneous label distribution (Berendt

et al. 2020). We suggest conducting pre-tests to determine the best moisture conditions for the labelling of each experimental site. NO_3^- -N and especially NH_4^+ -N concentrations found in the samples do not correspond with their ^{15}N recovery rates (Table 2). The comparably high NH_4^+ -N concentrations in soil samples after the sprinkler application are probably caused by local hare excrements which affect one sample.

The drip application achieved significantly larger $^{15}\text{N-NO}_3^-$ and $^{15}\text{N-NH}_4^+$ recovery rates than the sprinkler application in the top 0–2.5 cm soil layer (Fig. 5C, 5D). In deeper layers, as expected from blue dye pretests, the recovery rate of all methods declined. This led to vertical inhomogeneity with mean recovery rates of the drip application not significantly larger than those of the sprinkler application. Yet the drip application recovery rates were more reliable, shown by smaller CVs for separate depths (except $^{15}\text{N-NO}_3^-$ in 7.5–10 cm).

$^{15}\text{N-NO}_3^-$ label distribution can be further optimized by applying larger volumes (Berendt et al. 2020) and extending the application time. However, very long application times can also lead to evaporation losses of the supplied solution (Crouse et al. 1966; Schneider 2000) and conversion of the label, likely negatively impacting label distribution. To resolve the vertical decline of $^{15}\text{N-NO}_3^-$, water can be applied afterwards, ideally also using the drip application. However, when both $^{15}\text{N-NO}_3^-$ and $^{15}\text{N-NH}_4^+$ labels are applied, different mobility of NO_3^- and NH_4^+ (Sollins et al. 1988) would augment local division between both labels, as confirmed with our experiments (Fig. 5C, 5D). This can result in $^{15}\text{N}_2\text{O}$ originating from different soil depths with both different soil conditions and isotopic labelling, making the identification and differentiation of underlying processes of N_2O production much more difficult.

We conducted our comparative experiment with a clayey soil, which presents rather difficult conditions for a homogeneous labelling. In a sandier soil, infiltration rates are generally higher and therefore the influence of macropores on infiltration heterogeneity is lower. The application of labels should therefore lead to a more homogeneous distribution. It is possible that the difference between the methods we have compared would be less significant, but at the same time the drip application method should not be inferior to the comparative method, as the properties that lead to a better distribution (i.e. reduction of macropore flow) are still present.

Table 3 provides an overview of important factors affecting the label application in the field comparing the two methods in our experiments with a multi-injector method and a watering can application. The latter needs even less preparation than the sprinkler application and less labour input for application. It is a simple method and very fast. Because of the broad application of labelling, it is not very flexible when it comes to using different labels for different

Table 3 Overview of important factors in application of labels in the field evaluated for drip application (DA) and sprinkler application (SA) of our experiments as well as for application with a watering can (WC) based on Berendt et al. (2020) and a multi-injector method (MI) based on Wang et al. (2016). “Size S”: small plots < 1m² and “Size L”: large plots > 1m². +(+): (much) better than o, -(-): (much) worse than o.

Factor	Size	DA	SA	WC	MI
Workload for preparation	S	o	++	++	-
	L	-	++	++	o
Workload for application	S	o	o	+	o
	L	-	-	O	-
Method complexity	S	o	+	++	--
	L	o	+	++	--
Application speed	S	o	+	++	-
	L	o	-/+*	+	--
Flexibility	S	o	o	-	-/+**
	L	o	-	--	-/+**
User bias	S	o	-	-	o
	L	o	-/-*	-/-**	o
Robustness		o	o	O	--
Recovery		o	-	--	o
Horizontal homogeneity		o	-	--	o
Vertical homogeneity		o	-	--	++
Invasiveness		o	o	O	--

*Multiple applicators increase application speed and user bias

**Flexibility of MI is increased when individual multi-injector plates with different cannula distributions are prepared, but complexity and preparation required increase.

areas and, as with the sprinkler application, different users can introduce bias. Since application is even faster than with the sprinkler application, the overhead pressure will be larger, promoting even more preferential flow (Jarvis 2007). This should result in a less homogenous infiltration than with the sprinkler application and therefore less homogeneous label distribution.

A multi-injector method as suggested by Wang et al. (2016) for intact soil cores would be the only method considered that could lead to a vertically more homogeneous application than the drip application, especially for ¹⁵N-NH₄⁺ label. For the comparison in Table 3, we defined some additional characteristics for the multi-injector, based on our experiences gained so far. With the multi-injector, label also needs to be applied slowly to avoid preferential flow to deeper soil layers (Berendt et al. 2020).

Therefore, application is similarly fast as the drip application for areas as large as the multi-injector, but much slower for larger areas. Application with cannulas should start from the top to avoid preferential flow through the macropore created. The flow rate through each cannula should be fixed.

These requirements, including the necessary precision and rigidity of a multi-cannula application plate, result in a very complex system. Obstacles like stones or roots might lead to bending of the cannulas or non-applicability of the method, thereby restricting it to certain soil environments. Additionally, an artificial macropore created by the cannulas cause changes in soil gas diffusivity. Balaine et al. (2013) showed that relative gas diffusivity is an effective soil variable defining maximum N₂O emissions for different soils. Macropores facilitate the diffusion of N₂O out and of O₂ into the soil-cores (Balaine et al. 2013). Any mingling with this would counteract the quantification of N₂O emissions from soils under natural conditions.

To conclude, our experiments have revealed that drip application of ¹⁵N-labelled mineral N is a suitable *in-situ* method at the plot level and the best among the different methods tested. Drip application enhanced the ¹⁵N recovery rate, the horizontal and to a certain extent also the vertical homogeneity of label distribution and provided flexibility in terms of required application pattern and small-scale different ¹⁵N label application compared to existing methods. At the same time, the personal influence of the user was kept low without making the method too complex and difficult to use.

Supplementary Information The online version contains supplementary material available at <https://doi.org/10.1007/s00374-023-01730-8>.

Acknowledgments We thank Nicol Strasilla, Gerhard Mayer and Diana Werner for skillful help in the laboratories and in the field. The study was funded by the Deutsche Forschungsgemeinschaft (DFG) through the research unit DFG-FOR 2337 `Denitrification in Agricultural Soils: Integrated control and Modelling at various scales (DASIM)` (grants WR211/1-2 and MU1302/11-2).

Funding Open Access funding enabled and organized by Projekt DEAL.

Data availability The data that support the findings of this study are openly available in JLUpub at <https://doi.org/10.22029/jlupub-15694>.

Declarations

Conflicts of interest The authors have no conflicts of interest to declare that are relevant to the content of this article.

Open Access This article is licensed under a Creative Commons Attribution 4.0 International License, which permits use, sharing, adaptation, distribution and reproduction in any medium or format, as long as you give appropriate credit to the original author(s) and the source, provide a link to the Creative Commons licence, and indicate if changes were made. The images or other third party material in this article are included in the article's Creative Commons licence, unless indicated otherwise in a credit line to the material. If material is not included in the article's Creative Commons licence and your intended use is not permitted by statutory regulation or exceeds the permitted use, you will need to obtain permission directly from the copyright holder. To view a copy of this licence, visit <http://creativecommons.org/licenses/by/4.0/>.

References

- Anderson JL, Bouma J (1977) Water movement through pedal soils II. Unsaturated flow. *Soil Sci Soc Am J*:419–423. <https://doi.org/10.2136/sssaj1977.03615995004100020050x>
- Balaine N, Clough TJ, Beare MH, Thomas SM, Meenken ED, Ross JG (2013) Changes in relative gas diffusivity explain soil nitrous oxide flux dynamics. *Soil Sci Soc Am J* 77:1496–1505. <https://doi.org/10.2136/sssaj2013.04.0141>
- Barnard R, Leadley PW, Lensi R, Barthes L (2005) Plant, soil microbial and soil inorganic nitrogen responses to elevated CO₂: a study in microcosms of *Holcus lanatus*. *Acta Oecologica* 27:171–178. <https://doi.org/10.1016/j.actao.2004.11.005>
- Berendt J, Tenspolde A, Rex D, Clough TJ, Wrage-Mönnig N (2020) Application methods of tracers for N₂O source determination lead to inhomogeneous distribution in field plots. *Anal Sci Adv* 1:221–232. <https://doi.org/10.1002/ansa.202000100>
- Bethune MG, Selle B, Wang QJ (2008) Understanding and predicting deep percolation under surface irrigation. *Water Resour Res* 44. <https://doi.org/10.1029/2007WR006380>
- Bowden WB (1986) Gaseous nitrogen emissions from undisturbed terrestrial ecosystems: an assessment of their impacts on local and global nitrogen budgets. *Biogeochem* 1986:249–279. <https://doi.org/10.1007/BF02180161>
- Brooks PD, Stark JM, McInteer BB, Preston T (1989) Diffusion method to prepare soil extracts for automated nitrogen-15 analysis. *Soil Sci Soc Am J* 1989:1707–1711. <https://doi.org/10.2136/sssaj1989.03615995005300060016x>
- Buchen C, Lewicka-Szczebak D, Fuß R, Helfrich M, Flessa H, Well R (2016) Fluxes of N₂ and N₂O and contributing processes in summer after grassland renewal and grassland conversion to maize cropping on a Plagic Anthrosol and a Histic Gleysol. *Soil Biol Biochem* 101:6–19. <https://doi.org/10.1016/j.soilbio.2016.06.028>
- Corbett ES, Crouse RP (1968) Rainfall interception by annual grass and chaparral . . . losses compared. U.S.D.A. Forest Serv Res Note PSW-RP 48:1–12. https://www.fs.usda.gov/psw/publications/documents/psw_rp048/psw_rp048.pdf. Accessed 19 Dec 2022
- Crouse RP, Corbett ES, Seegrift DW (1966) Methods of measuring and analyzing rainfall interception by grass. *Hydrol Sci J* 11:110–120. <https://doi.org/10.1080/02626666609493463>
- Davidson EA, Hart SC, Shanks CA, Firestone MK (1991) Measuring gross nitrogen mineralization, and nitrification by ¹⁵N isotopic pool dilution in intact soil cores. *J Soil Sci* 42:335–349. <https://doi.org/10.1111/j.1365-2389.1991.tb00413.x>
- Doerr SH, Shakesby RA, Walsh RPD (2000) Soil water repellency: its causes, characteristics and hydro-geomorphical significance. *Earth-Sci Rev*:33–65. [https://doi.org/10.1016/S0012-8252\(00\)00011-8](https://doi.org/10.1016/S0012-8252(00)00011-8)
- Elrick DE, French LK (1966) Miscible displacement patterns on disturbed and undisturbed soil cores. *Soil Sci Soc Am J*:153–156. <https://doi.org/10.2136/sssaj1966.03615995003000020007x>
- Flühler H, Durner W, Flury M (1996) Lateral solute mixing processes - A key for understanding field-scale transport of water and solutes. *Geoderma*:165–183. [https://doi.org/10.1016/0016-7061\(95\)00079-8](https://doi.org/10.1016/0016-7061(95)00079-8)
- Flury M, Flühler H (1994) Brilliant Blue FCF as a Dye Tracer for Solute Transport Studies-A Toxicological Overview. *J Environ Qual* 23:1108–1112. <https://doi.org/10.2134/jeq1994.00472425002300050037x>
- Hartmann DL, Klein Tank AM, Rusticucci M, Alexander LV, Brönnimann S, Charabi Y, Dentener FJ, Dlugokencky EJ, Easterling DR, Kaplan A, Soden BJ, Thorne PW, Wild M, Zhai PM (2013) Observations: Atmosphere and Surface. *Climate Change*. Cambridge University Press, Cambridge, United Kingdom and New York, NY, USA, pp 159–254
- Heil J, Liu S, Vereecken H, Brüggemann N (2015) Abiotic nitrous oxide production from hydroxylamine in soils and their dependence on soil properties. *Soil Biol Biochem*:107–115. <https://doi.org/10.1016/j.soilbio.2015.02.022>
- Jäger H-J, Schmidt SW, Kammann C, Grünhage L, Müller C, Hanewald K (2003) The university of Giessen free-air carbon dioxide enrichment study: description of the experimental site and of a new enrichment system. *J Appl Bot*:117–127
- Jarvis NJ (2007) A review of non-equilibrium water flow and solute transport in soil macropores: principles, controlling factors and consequences for water quality. *Soil Sci* 58:523–546. <https://doi.org/10.1111/j.1365-2389.2007.00915.x>
- Ketelsen H, Meyer-Windel S (1999) Adsorption of brilliant blue FCF by soils. *Geoderma* 90:131–145. [https://doi.org/10.1016/S0016-7061\(98\)00119-0](https://doi.org/10.1016/S0016-7061(98)00119-0)
- King BA, Bjorneberg DL (2011) Evaluation of potential runoff and erosion of four center pivot irrigation sprinklers. *J ASABE* 27:75–85. <https://doi.org/10.13031/2013.36226>
- Kinnersley RP, Goddard AJH, Minski MJ, Shaw G (1997) Interception of cesium-contaminated rain by vegetation. *Atmos Environ* 31:1137–1145. [https://doi.org/10.1016/S1352-2310\(96\)00312-3](https://doi.org/10.1016/S1352-2310(96)00312-3)
- Kool DM, van Groenigen JW, Wrage N (2011) Source determination of nitrous oxide based on nitrogen and oxygen isotope tracing dealing with oxygen exchange. *Methods Enzymol* 496:139–160. <https://doi.org/10.1016/B978-0-12-386489-5.00006-3>
- Lewicka-Szczebak D, Well R (2020) The ¹⁵N gas-flux method to determine N₂ flux: a comparison of different tracer addition approaches. *SOIL* 6:145–152. <https://doi.org/10.5194/soil-6-145-2020>
- McLeod M, Schipper LA, Taylor MD (1998) Preferential flow in a well drained and a poorly drained soil under different overhead irrigation regimes. *Soil Use Manage*:96–100. <https://doi.org/10.1111/j.1475-2743.1998.tb00622.x>
- Moser G, Gorenflo A, Brenzinger K, Keidel L, Braker G, Marhan S, Clough TJ, Müller C (2018) Explaining the doubling of N₂O emissions under elevated CO₂ in the Giessen FACE via in-field ¹⁵N tracing. *Glob Chang Biol* 24:3897–3910. <https://doi.org/10.1111/gcb.14136>
- Müller C, Clough TJ (2014) Advances in understanding nitrogen flows and transformations: gaps and research pathways. *J Agric Sci* 152:34–44. <https://doi.org/10.1017/S0021859613000610>
- Müller C, Laughlin RJ, Spott O, Rütting T (2014) Quantification of N₂O emission pathways via a ¹⁵N tracing model. *Soil Biol Biochem* 72:44–54. <https://doi.org/10.1016/j.soilbio.2014.01.013>
- Nimmo JR (2012) Preferential flow occurs in unsaturated conditions. *Hydrol Process* 26:786–789. <https://doi.org/10.1002/hyp.8380>
- R Core Team (2021) R: a language and environment for statistical computing, Vienna, Austria. <https://www.Rproject.org/>. Accessed 19 Dec 2022
- Radulovich R, Sollins P, Solórzano E (1992) Bypass water flow through unsaturated microaggregated tropical soils. *Soil Sci Soc Am J*:721–726. <https://doi.org/10.2136/sssaj1992.03615995005600030008x>
- Ritsemá CJ, Dekker LW (1995) Distribution Flow: A General Process in the Top Layer of Water Repellent Soils. *Water Resour Res*:1187–1200. <https://doi.org/10.1029/94WR02979>
- Schneider AD (2000) Efficiency and uniformity of the LEPA and spray sprinkler methods: A review. *J ASABE* 43:937–944. <https://doi.org/10.13031/2013.2990>
- Sextone AJ, Revsbech NP, Parkin TB, Tiedje JM (1985) Direct measurement of oxygen profiles and denitrification rates in soil aggregates. *Soil Sci Soc Am J*:645–651. <https://doi.org/10.2136/sssaj1985.03615995004900030024x>
- Seyfried MS, Rao PSC (1987) Solute transport in undisturbed columns of an aggregated tropical soil: Preferential flow effects. *Soil Sci Soc Am J*:1434–1444. <https://doi.org/10.2136/sssaj1987.03615995005100060008x>

- Sgouridis F, Stott A, Ullah S (2016) Application of the ^{15}N gas-flux method for measuring in situ N_2 and N_2O fluxes due to denitrification in natural and semi-natural terrestrial ecosystems and comparison with the acetylene inhibition technique. *Biogeosciences* 13:1821–1835. <https://doi.org/10.5194/bg-13-1821-2016>
- Siegel RS, Hauck RD, Kurtz LT (1982) Determination of $^{30}\text{N}_2$ and application to measurement of N_2 evolution during denitrification. *Soil Sci Soc Am J*:68–74. <https://doi.org/10.2136/sssaj1982.03615995004600010013x>
- Sollins P, Robertson GP, Uehara G (1988) Nutrient Mobility in Variable- and Permanent-Charge Soils. *Biogeochem* 6:181–199. <https://doi.org/10.1007/BF02180161>
- Stein LY (2019) Insights into the physiology of ammonia-oxidizing microorganisms. *Curr Opin Chem Biol* 49:9–15. <https://doi.org/10.1016/j.cbpa.2018.09.003>
- Syakila A, Kroeze C (2011) The global nitrous oxide budget revisited. *Greenh Gas Meas Manage* 1:17–26. <https://doi.org/10.3763/ghgmm.2010.0007>
- Thompson RL, Lassaletta L, Patra PK, Wilson C, Wells KC, Gressent A, Koffi EN, Chipperfield MP, Winiwarter W, Davidson EA, Tian H, Canadell JG (2019) Acceleration of global N_2O emissions seen from two decades of atmospheric inversion. *Nat Clim Chang* 9:993–998. <https://doi.org/10.1038/s41558-019-0613-7>
- Thurrow TL, Blackburn WH, Warren SD, Taylor JR (1987) Rainfall Interception by Midgrass, Shortgrass, and Live Oak Mottes. *J Range Manage* 40:455–460. <https://doi.org/10.2307/3899611>
- Wang C, Chen Z, Unteregelsbacher S, Lu H, Gschwendtner S, Gasche R, Kolar A, Schloter M, Kiese R, Butterbach-Bahl K, Dannenmann M (2016) Climate change amplifies gross nitrogen turnover in montane grasslands of Central Europe in both summer and winter seasons. *Glob Chang Biol* 22:2963–2978. <https://doi.org/10.1111/gcb.13353>
- Well R, Burkart S, Giesemann A, Grosz B, Köster JR, Lewicka-Szczepak D (2019) Improvement of the ^{15}N gas flux method for in situ measurement of soil denitrification and its product stoichiometry. *Rapid Commun Mass Spectrom* 33:437–448. <https://doi.org/10.1002/rcm.8363>
- Wrage N, van Groenigen JW, Oenema O, Baggs EM (2005) A novel dual-isotope labelling method for distinguishing between soil sources of N_2O . *Rapid Commun Mass Spectrom* 19:3298–3306. <https://doi.org/10.1002/rcm.2191>
- Wrage-Mönnig N, Horn MA, Well R, Müller C, Velthof G, Oenema O (2018) The role of nitrifier denitrification in the production of nitrous oxide revisited. *Soil Biol Biochem* 123:A3–A16. <https://doi.org/10.1016/j.soilbio.2018.03.020>
- Wu H, Dannenmann M, Fanselow N, Wolf B, Yao Z, Wu X, Brüggemann N, Zheng X, Han X, Dittert K, Butterbach-Bahl K (2011) Feedback of grazing on gross rates of N mineralization and inorganic N partitioning in steppe soils of Inner Mongolia. *Plant Soil* 340:127–139. <https://doi.org/10.1007/s11104-010-0575-z>
- Zaman M, Kleineidam K, Bakken L, Berendt J, Bracken C, Butterbach-Bahl K, Cai Z, Chang CX, Clough T, Dawar K, Ding WX, Dörsch P, dos Reis Martins M, Eckhardt C, Fiedler S, Frosch T, Goopy J, Görres C-M, Gupta A, Henjes S, Hofmann ME, Horn MA, Jahangir MM, Jansen-Willems A, Lenhart K, Heng L, Lewicka-Szczepak D, Lucic G, Merbold L, Mohn J, Molstad L, Moser G, Murphy P, Sanz-Cobena A, Šimek M, Urquiaga S, Well R, Wrage-Mönnig N, Zaman S, Zhang J, Müller C (2021) Measuring Emission of Agricultural Greenhouse Gases and Developing Mitigation Options using Nuclear and Related Techniques. Springer International Publishing, Cham

Publisher's note Springer Nature remains neutral with regard to jurisdictional claims in published maps and institutional affiliations.